Calculated electronic and magnetic structure of the nitrides $NiFe_3N$ and $PdFe_3N$

P. Mohn and K. Schwarz
Institut für Technische Elecktrochemie, Technische Universität Wien, A-1060 Vienna, Getreidemarkt 9/158, Austria

S. Matar and G. Demazeau
Laboratoire de Chimie du Solide du CNRS, Université Bordeaux I, 351 cours de la Libération, 33405 Talence CEDEX, France

(Received 30 May 1991)

The electronic and magnetic structure of the antiperovskite-structure transition-metal nitrides $NiFe_3N$ and $PdFe_3N$ are calculated employing the augmented-spherical-wave method. From these calculations the binding character is found to be mainly covalent for the nitrogen-iron bonds and metallic between the iron and nickel atoms, as stated in the earlier literature. The magnetic structure exhibits itinerant moments for the iron atoms and more localized moments at the Ni (Pd) atoms. Effects of external pressure are studied by varying the lattice constant. Such calculations yield the pressure dependence of the magnetic moments and the hyperfine fields. The total energy is computed as a function of magnetic moment and volume, yielding total-energy surfaces, that provide the basis for a spin-fluctuation model at finite temperatures. The possibility of an Invar-like behavior is found.

I. INTRODUCTION

Although several studies have been reported on transition-metal iron nitrides MFe_3N (M=Fe, Ni, Pd, and Pt),[1-8] these systems merit further investigation. These compounds crystallize in the antiperovskite crystal structure (Fig. 1), which is simple enough to allow a first-principles investigation of the electronic and magnetic behavior. The properties of both the constituent atoms and bulk compound are of interest. Wiener and Berger[1] showed in their x-ray-diffraction experiments that $NiFe_3N$ and $PtFe_3N$ are ordered compounds with the nickel or platinum atom placed at the corner positions of the unit cell, as shown in Fig. 1. These early experiments have been corroborated by calculations of the x-ray line intensities[2] as well as by a phenomenological interpretation of the electronic configuration of Ni and Fe in $NiFe_3N$.[3] Mössbauer measurements comparing Fe_4N and $NiFe_3N$ (Refs. 4 and 5) showed, however, that at least 80% of the Ni atoms are in the corner position (see Fig. 1) so that a modeling of $NiFe_3N$ by the ordered structure seems justified. In 1960 Stadelmaier and Fraker[7] isolated an isostructural nitride $PdFe_3N$, which is closely related to the Ni analog. Mössbauer experiments[8] for $PdFe_3N$ and $PtFe_3N$ have shown that both compounds are completely ordered. Ferromagnetic spin alignment has been found for all those iron nitrides in contrast to the manganese-based nitrides which exhibit ferrimagnetism.[1]

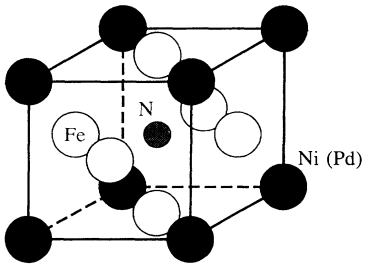

FIG. 1. Antiperovskite structure of $NiFe_3N$ ($PdFe_3N$): with the Ni (Pd) atoms at the corner (solid circles), the Fe atoms at the face center (open circles), and the nitrogen position (hatched circle).

Recent investigations[9] of the thermal expansion and forced magnetostriction of $NiFe_3N$ observed similarities to the Fe-Ni Invar alloys. It was shown that the thermal-expansion coefficient (at room temperature) of $NiFe_3N$ is relatively small and is significantly smaller than that of Fe_4N, but is not as close to zero as that of the Invar alloy $Fe_{65}Ni_{35}$. Moreover, measurements of the forced magnetostriction have shown that the variation of volume with magnetic field or of magnetization with pressure is rather similar between $NiFe_3N$ and $Fe_{65}Ni_{35}$.

Band-theoretical investigations in this class of compounds have been undertaken by Matar *et al.*,[10] employing the augmented-spherical-wave (ASW) method of Williams, Kübler, and Gelatt.[11] For the two compounds Fe_4N and Mn_4N, these calculations gave results in good agreement with experimental findings concerning the value and orientation of the magnetic moments.

In the present work, the same method is applied to the two systems $NiFe_3N$ and $PdFe_3N$, but in order to obtain information about the magnetomechanical properties, the calculations are extended to compute the total energy as a function of volume and magnetic moment, employing the fixed-spin-moment (FSM) method.[12,13] It has been shown for Fe-Ni Invar alloys that with such FSM energy surfaces one can include spin fluctuations on the basis of a Landau-Ginzburg[14,15] theory, which allows one to describe the finite-temperature behavior of the magnetic and related mechanical properties.

II. ASW METHOD AND COMPUTATIONAL DETAILS

The ASW method[11] is a first-principles method for self-consistently calculating the band structure of solids.

The calculations are based on local-spin-density-functional theory in which we treat exchange and correlation effects using the parametrization of von Barth and Hedin[16] and Janak.[17] The Brillouin-zone integration is carried out for 56 k points in an irreducible wedge. The matrix elements are constructed using partial waves to up $l=2$ (s, p, and d states) for the transition metals and up to $l=1$ (s and p states) for nitrogen. A contribution associated with the term with $l+1$ includes corrections due to the internal summation over the three center integrals. The calculations are carried to self-consistency, which is monitored by the site- and l-projected partial charges, which converged better than 0.0001 electron. The effect of magnetic ordering is made possible by allowing spin polarization. In the ASW method the atomic-sphere approximation (ASA) is used, in which each atom is surrounded by a sphere. Inside each sphere the potential and charge density is assumed to be spherically symmetric; the space outside the spheres is neglected, but the sum of volumes of all (overlapping) spheres equals the volume of the unit cell. The ASA, although approximate, allows one to decompose various quantities of interest into atomic contributions and thus simplifies the interpretation, but it should be kept in mind that this decomposition depends on the choice of sphere radii and therefore is model dependent.

The perovskite structure for $NiFe_3N$ and $PdFe_3N$ is shown in Fig. 1, but since the lattice constant is rather large, the structure becomes open and poorly packed. This circumstance, in combination with the ASA, led us to introduce 12 empty spheres—pseudoatoms with atomic number $Z=0$—centered at all edges of the cube shown in Fig. 1. These spheres contain the "tails" of the wave functions from the neighboring spheres and thus mediate between atoms which otherwise would be too far apart from their spheres to overlap. For the smallest lattice constant ($a_0=6.377\,65$ a.u.), the following sphere radii are used: 2.401 56 a.u. for the metal atoms and 1.639 12 a.u. for the nitrogen and empty spheres. The ratio of the sphere volumes is kept constant for the other lattice constants as well. The additional empty spheres allow one to reduce the otherwise large overlap between adjacent atomic spheres, but should not affect the results much in a metallic system.

In the FSM method,[12,13] one performs constraint self-consistent calculations in which the magnetic moment is specified as the input parameter. This method leads to two Fermi energies (for spin-up and -down electrons) which coincide for equilibrium states.

III. CALCULATIONS AND RESULTS

First, we perform self-consistent FSM calculations for both compounds, where four different lattice spacings (corresponding to volume V) are taken and the magnetic moment M is varied from 0 to $10\mu_B$/unit cell in steps of 1. The respective total energies are fitted to an analytic expression representing the energy surface, $E(M,V)$, as has been described previously.[15] In this representation the total energy is easily minimized to yield the theoretical equilibrium values for the lattice constant and magnetic moment. In both compounds the ferromagnetic state is found to be more stable than the nonmagnetic one. Tables I and II contain three types of results and their variation with lattice spacings: (i) the density of states at the Fermi energy, $N(E_F)$, (ii) the magnetic moments at various sites, M, and (iii) the site-projected charges q.

TABLE I. Band-structure results for $NiFe_3N$ at four different lattice constants: DOS↑ and DOS↓ are the spin-projected densities of states at E_F for spin-up and -down electrons in states per Ry and formula unit (f.u.); $M(i)$ and M(f.u.) are the magnetic moments at site i and per f.u.; $q(i)$ are the spin- and site-projected total charges, where ES refers to empty spheres.

a_0 (a.u.)	7.375 69	7.160 86	6.946 03	6.737 65
DOS↑ (Ry^{-1})	10.76	37.77	22.19	32.38
DOS↓ (Ry^{-1})	59.29	59.97	63.11	46.59
M(Ni)/μ_B	0.84	0.86	0.90	0.90
M(Fe)/μ_B	2.47	2.16	1.52	1.17
M(N)/μ_B	0.05	0.03	−0.04	−0.04
M(f.u.)/μ_B	8.23	7.32	5.28	4.33
q(Ni)↑	5.169	5.163	5.157	5.143
q(Ni)↓	4.330	4.301	4.262	4.239
q(Fe)↑	5.126	4.978	4.666	4.490
q(Fe)↓	2.659	2.817	3.145	3.325
q(N)↑	2.293	2.244	2.163	2.128
q(N)↓	2.243	2.217	2.207	2.171
q(ES)↑	0.258	0.273	0.289	0.307
q(ES)↓	0.278	0.291	0.304	0.318

With the present choice of sphere radii, there is only a small charge transfer, which does not change drastically with volume, but we want to point out that the assumption to keep the ratio of the atomic-sphere volumes constant could affect the charge transfer. Both atoms Ni (Pd) and Fe have a charge density which extends into the empty spheres. However, the main contributors are the Ni (Pd) atoms at the corner of the unit cell. The Ni (Pd) t_{2g} states interact with those of the iron atoms at the face-centered positions forming $dd\sigma$ bonding and anti-

TABLE II. Band-structure results for $PdFe_3N$ at four different lattice constants (see Table I).

a_0 (a.u.)	7.375 69	7.160 86	6.946 03	6.737 65
DOS↑ (Ry^{-1})	10.39	32.81	21.33	65.85
DOS↓ (Ry^{-1})	48.31	59.76	59.66	34.16
M(Pd)/μ_B	0.44	0.45	0.46	0.33
M(Fe)/μ_B	2.54	2.20	1.63	1.07
M(N)/μ_B	0.05	0.02	−0.04	−0.04
M(f.u.)/μ_B	8.07	7.03	5.30	3.47
q(Pd)↑	4.796	4.758	4.713	4.587
q(Pd)↓	4.368	4.307	4.250	4.257
q(Fe)↑	5.188	5.028	4.761	4.490
q(Fe)↓	2.649	2.833	3.127	3.423
q(N)↑	2.294	2.241	2.168	2.130
q(N)↓	2.241	2.217	2.203	2.168
q(ES)↑	0.294	0.311	0.329	0.350
q(ES)↓	0.305	0.321	0.339	0.356

bonding states.

The e_g states of Ni (Pd) point toward the empty spheres, which are along the edges of the unit cell (Fig. 1) and octahedrally surround the (Pd) atoms. These e_g states hardly interact with the respective states of the neighboring Ni (Pd) atoms because of the large separation between them. This bonding mechanism explains why these e_g states form narrow bands and cause most of the charge inside the empty spheres.

A. Densities of states

Figures 2 and 3 show the site- and spin-projected densities of states (DOS) for $NiFe_3N$ and $PdFe_3N$. The top panels contain the DOS of iron (solid curve) and those of nitrogen (dotted curve) and indicate a strong interaction between the Fe $3d$ and N $2p$ orbitals. Some features are important and are discussed below: For example, the spin-up DOS peaks near -8 and 3 eV correspond to σ and σ^* bonds, respectively, while those near -6 and 0 eV come from N p–Fe d π bonding and π^* antibonding states. The N $2s$ states are included in the calculation as valence states, but they are omitted in Figs. 2 and 3 since these electrons form a narrow band showing little interaction with other states. The bottom panel of Fig. 2 (Fig. 3) shows the DOS of Ni (Pd), which is large in the same energy range as that of iron. The interactions between the two metal sublattices, namely, Ni (Pd) and Fe, can be interpreted in terms of *covalent magnetism*.[18] An explanation of this class of compounds has been given by Goodenough.[19]

The electronic structures of $NiFe_3N$ and $PdFe_3N$ have many features in common, so that we start out describing the $NiFe_3N$ system. The bonding mechanism and its relation to the magnetic behavior will be simplified below in order to focus on two important aspects: First, we consider the interaction between N and Fe and, second, the metallic bonds between Fe and Ni (Pd). The Fe-N interaction has a strong covalent character, with an obvious bond between one $3d$ -electron in an e_g orbital (d_{z^2}) of the iron atom (at the face-centered position) and one of the three $2p$ electrons (p_z) of nitrogen (forming a σ bond). The Fe t_{2g} orbitals remain mostly nonbonding with respect to the Fe-N bond except the weak π bond, which—as an example—occurs between a N p_x and a Fe d_{xz} orbital (Fig. 4). The antibonding π^* lies above the main d DOS and just near E_F for the spin-up case. This π^* DOS near E_F is responsible for making the system a weak itinerant ferromagnet and is missing in the nitrogen-free system, so that this part of the DOS is essential for understanding the magnetic behavior. With the configuration assumed above, one Fe e_g electron is spin paired with the N $2p$ electron when forming the Fe-N σ bond. The formation of this bond reduces the number of d electrons which can develop a magnetic moment

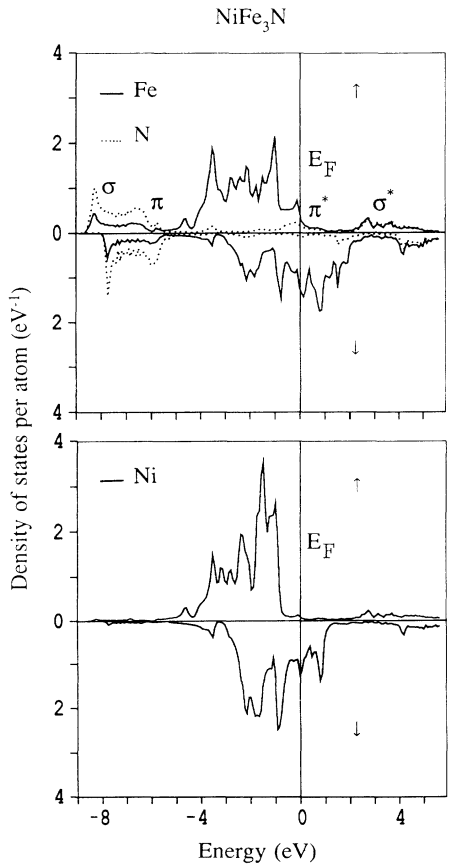

FIG. 2. Site- and spin-decomposed densities of states (DOS) of $NiFe_3N$ for the equilibrium volume.

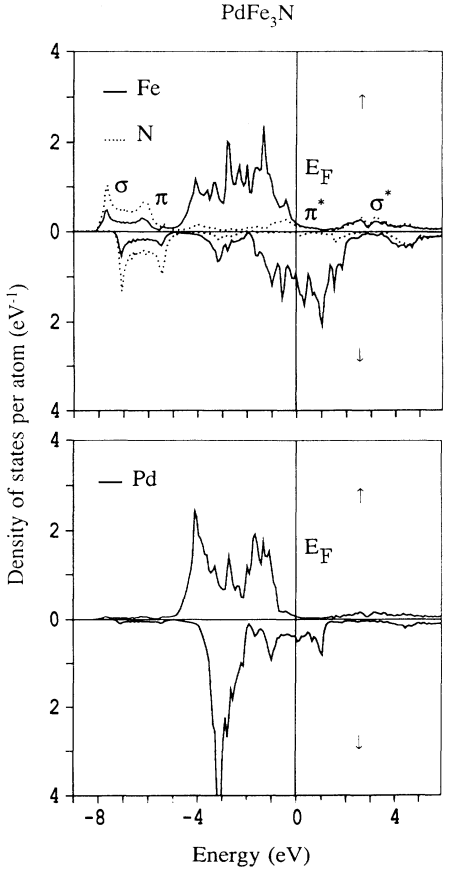

FIG. 3. Site- and spin-decomposed densities of states (DOS) of $PdFe_3N$ for the equilibrium volume.

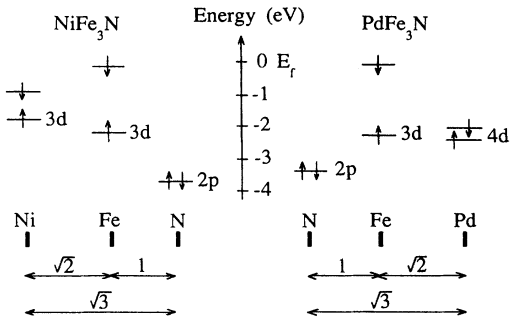

FIG. 4. Atomic-orbital diagram for the possible interactions between nitrogen, iron, and Ni (Pd) in $NiFe_3N$ and $PdFe_3N$. At the bottom the interatomic distances are given in units of half the lattice constant. For an explanation, see text.

at the respective iron site. This situation is similar to Fe_4N, where the magnetic moments differ by about $1\mu_B$ between the corner and face-centered position.[10]

The metallic interaction between the two metal sublattices is well explained within the model of covalent magnetism[18] and is similar to Fe_4N as described in Ref. 10. The center of gravity of the bands is given by the Hankel energies within the ASW formalism.[11] By taking these from the self-consistent ASW calculation, we obtain an atomic-orbital diagram (Fig. 4) which shows the energy positions of all the essential orbitals involved. The d orbitals of Fe show a much larger exchange splitting than those of Ni (Pd) but the N p orbitals show none. Considering that the Fe-N, Fe-Ni, and Ni-N distances (in units of half the lattice constant) are proportional to 1, $\sqrt{2}$, and $\sqrt{3}$, respectively, we have all the ingredients to describe qualitatively the DOS.

The nearest neighbors Fe and N form a strong σ and σ^* and a weaker π and π^* bond, while Ni (Pd) interacts little with N since they are too far apart. For the second-nearest neighbors (e.g., Fe and Ni), the spin-up orbitals are close in energy and thus lead to a *common band* with a DOS comparable to that of a fcc transition metal. In the spin-down case, however, especially for Pd, the energy separation to Fe d is so large that we find more of a *split band* behavior where in the bonding part the DOS has a high Pd contribution with an admixture of Fe states, while in the antibonding energy region the relative weights between Pd and Fe are reversed.

It is of interest to study what happens when the nitrogen atom is removed from the compounds of investigation leading to Fe_3Ni in the Cu_3Au structure. In order to find the influence of nitrogen, we performed two calculations for Fe_3Ni, with one taking its own equilibrium lattice constant and the other by expanding it to the same volume as that of $NiFe_3N$. In the former case, one obtains a very weak itinerant ferromagnet where the Fermi energy lies in the spin-up d band of both Fe and Ni; this Fe_3Ni allows one to describe the Invar behavior of the Fe-Ni alloy,[15] as it comes close to the actual $Fe_{65}Ni_{35}$ Invar composition. In the latter case (the lattice constant is increased by 7%), we find a strong itinerant ferromagnet where the Fermi energy is above the spin-up d band of both constituents.

This finding contrasts the result shown in Figs. 2 and 3, where the Fermi energy is still inside the spin-up d band of Fe. As analyzed above, the Fe-N interactions lead to states at the bottom and top of the Fe d band (bonding and antibonding states). They cause the weak itinerant behavior of the nitrogen-containing compound and are responsible for the Invar-like behavior[9] of $NiFe_3N$. The shape of the Ni DOS is not much affected upon the insertion of nitrogen and thus looks rather similar for $NiFe_3N$ and Fe_3Ni when results for the same lattice constants are compared.

B. Influence of pressure on the magnetization

In the investigation of Fe_4N and Mn_4N, as has already been pointed out,[10] there is a similarity in the magnetic behavior between the present class of transition-metal nitrides and the Heusler alloys.[20] In both systems one finds a pronounced deviation from rigid-band behavior, at least for one of the constituent metals. This becomes especially apparent for the Pd spin-down d band, which is much narrower than the spin-up counterpart. Nevertheless, the moments in the present systems are all due to itinerant electrons. One expects different pressure behavior of the Fe and Ni (Pd) moments.

In Stoner theory there is always a critical pressure for the disappearance of magnetism. Applying pressure makes the interaction stronger, so that the dispersion of the bands and consequently the bandwidth increases while the average DOS decreases. Eventually, the DOS at the Fermi energy will drop below the critical value required to fulfill Stoner's criterion, so that magnetism breaks down. In MFe_3N (M=Ni and Pd), the decrease of the total magnetization under pressure is mainly due to Fe, while the Ni or Pd moments slightly increase (except for Pd at the smallest lattice constant listed in Table II). The existence of different pressure dependencies of the metal sublattices has several reasons. Iron shows weak itinerant magnetism, which accounts for the sensitivity to variations in volume. The spin-up d bands of the Ni (Pd) sublattice, however, are fully occupied and thus correspond to a strong ferromagnet. In this case it is well established that the pressure dependence of the magnetic moment is much smaller than for weak itinerant magnets. The magnetic moments originating from the Ni (Pd) d electrons resemble those of the Heusler alloys[20] with rather localized d states, so that we expect their moments to be independent of pressure. The present calculations show that these d electrons produce a magnetic moment which remains almost constant near the equilibrium volume and has the values $0.94\mu_B$ and $0.51\mu_B$ for Ni and Pd, respectively (Table II). The total Ni (Pd) moment rises slightly under pressure (Tables I and II), an unusual behavior that calls for an explanation, which we give below for the Ni case (for $a_0=7.16$ a.u.).

The Ni moment of $0.86\mu_B$ can be decomposed into the large contribution from the d electrons ($0.94\mu_B$) and the antiparallel moment coming from the s and p electrons of $-0.08\mu_B$. This negative Ni sp moment stems partly from the intra-atomic polarization to the Ni d moment, but partly from the neighboring Fe atoms with their large magnetic moment (interatomic polarization). Analysis of

TABLE III. Calculated magnetic moments and hyperfine fields of the different sites in $NiFe_3N$ (top) and $PdFe_3N$ (bottom): M_d is the magnetic moment (in μ_B) produced by the d electrons; the hyperfine fields (in kG) are given as H_c from the core, H_v from the valence s electrons, and H_{hf} for the total.

$NiFe_3N$		Fe				Ni			N
a_0	M_d	H_c	H_v	H_{hf}	M_d	H_c	H_v	H_{hf}	H_{hf}
7.375 69	2.46	−249	79	−170	0.94	−100	−237	−337	−25
7.160 86	2.16	−216	42	−174	0.94	−100	−186	−286	−21
6.946 03	1.53	−150	−12	−162	0.95	−100	−116	−216	−14
6.737 65	1.18	−114	−16	−130	0.94	−98	−79	−177	−8
$PdFe_3N$		Fe				Pd			N
a_0	M_d	H_c	H_v	H_{hf}	M_d	H_c	H_v	H_{hf}	H_{hf}
7.375 69	2.52	−255	100	−155	0.50	−81	−414	−495	−17
7.160 86	2.19	−218	52	−163	0.51	−81	−336	−417	−14
6.946 03	1.64	−161	−1	−162	0.51	−81	−242	−323	−8
6.737 65	1.07	−103	−12	−115	0.36	−56	−159	−217	−8

hyperfine fields (see next section) indicates that the negative *sp* polarization is mainly caused by iron. Upon pressure the Ni *d* moment remains about constant (Table III), while the Fe moment decreases significantly (Tables I and II). The smaller iron moment induces a reduced negative *sp* polarization on Ni, which, together with the constant Ni *d* moment, leads to a slight increase of the total Ni moment.

C. Pressure dependence of the hyperfine fields

The hyperfine field at the two transition-metal sites varies differently under pressure and thus contrasts the behavior of pure transition metals, a challenge for theorists to provide an interpretation. In the following analysis we represent the hyperfine field by the most important contribution, namely, the nonrelativistic Fermi contact term which is proportional to the difference in the *s*-electron density at the nucleus between the two spin directions. The orbital contribution is often quenched in transition-metal compounds and is therefore completely neglected here.

In this approximation the total hyperfine field can be decomposed into contributions due to the core and valence *s* electrons, H_c and H_v, respectively (Table III). H_c is an intra-atomic quantity whose proportionality to the magnetic moment of the *d* electrons is called core polarization. For 3*d* metals the valence-electron contribution H_v can be small (typically of the order of $\cong 5\%$ of H_c), but not in the present case, where H_v is relatively large at both metal sites; for Ni and Pd, sometimes H_v dominates over H_c and is not proportional to the magnetic moment of the *d* electrons at the respective sites. For the iron atoms, H_v is relatively small and even changes sign under pressure. This variation produces a maximum of the total hyperfine field around the equilibrium lattice constant and leads to a smaller pressure dependence of the hyperfine field $\partial \ln H_{hf}/\partial P$ than that of the magnetic moment $\partial \ln M/\partial P$. A similar anomaly has been reported[21] for the hyperfine field at the yttrium site in the cubic Laves phase YFe_2: Although the magnetic moments at both the iron and yttrium sites decrease with increasing pressure, H_{hf} increases at the yttrium site, a behavior interpreted as a transferred hyperfine field. Recent Mössbauer studies of $NiFe_3N$ (Ref. 5) and $PdFe_3N$ (Ref. 8) found a hyperfine field of about 200 kG at the iron position. At the Ni (Pd) site, the valence contribution H_v varies and is much larger than H_c, which is almost independent of pressure as the corresponding magnetic moment.

The valence contributions H_v at the Ni (Pd) sites is proportional to the magnetic moment at the neighboring iron atoms, so that we can call it *transferred* in the sense that the Ni valence *s* electrons are polarized by the neighboring Fe *d* moments via a Ruderman-Kittel-Kasuya-Yosida-like mechanism. This interaction leads to an oscillating spin density of the *s* electrons and can be responsible for the change in sign of H_v at the iron sites.

The hyperfine field at the nitrogen nucleus is mainly influenced by the octahedrally surrounded iron atoms and thus follows their magnetic moments. From this analysis we conclude that the *s* electrons behave like free electrons and thus can easily be polarized by the atoms carrying *d* moments. This feature is even more true for the Ni (Pd) atoms, for which the on-site *s-d* interaction is weak, so that the *s* electrons can easily follow the polarization of the itinerant *d* electrons of the neighboring iron atoms.

IV. MAGNETOVOLUME EFFECTS IN $NiFe_3N$

The parent compound to the Fe-Ni nitride is ordered Fe_3Ni in the Cu_3Au phase, which is close to the Fe-Ni Invar composition $Fe_{65}Ni_{35}$. The latter was already reported in 1897 by Guillaume,[22] who found that the thermal-expansion coefficient of that alloy is very small near room temperature. This, however, is not the only anomalous behavior observed, but several related effects occur, such as a maximum in the volume, a minimum in the bulk modulus, a strong pressure dependence of the magnetization, Curie temperature, etc.

Band-structure calculations on Fe_3Ni have shown[14]

that this compound can be characterized by the following features: (i) a large difference in volume between the paramagnetic and ferromagnetic states, (ii) a small energy difference between the paramagnetic and ferromagnetic states, and (iii) strong magnetovolume coupling.

By applying a spin-fluctuation theory to this class of compounds,[14,15] one obtains a qualitative and quantitative description of the thermomagnetic and magnetomechanical properties. Such an investigation is based on FSM calculations, providing the total energy as a function of volume and magnetization. These energy surfaces are fitted by a polynomial in powers of the bulk magnetization M and bulk volume V. The simplest possible form of this polynomial is given by

$$E(M,V)=AM^2+BM^4+E_0+\beta V+\gamma V^2+\delta VM^2 . \quad (1)$$

The advantage of this simple form is that all parameters have a physical meaning: A and B can be taken from the Landau theory of itinerant ferromagnets, β and γ are related to the bulk modulus and the equilibrium volume in the paramagnetic state, and δ is the magnetovolume coupling constant.

This spin-fluctuation model relies on the fact that the longitudinal and transverse fluctuations of the systems are equal in magnitude, since one can only calculate the $T=0$ K energy of perfectly ordered magnetic moments. Also, this assumes that the Landau expansion performed at low temperatures (for M and V) is valid for spin fluctuations at high temperatures, where the magnetization also fluctuates transversely. The justification of this approach was demonstrated for the Fe-Ni Invar system.[14,15]

The FSM total-energy surfaces are shown in Figs. 5 and 6 and are fitted according to Eq. (1) to obtain the parameters given in Table IV. It has been shown[23] that such a fit describes the FSM surfaces well for the relevant volume and moment range. We find that both compounds have a rather strong magnetovolume coupling,

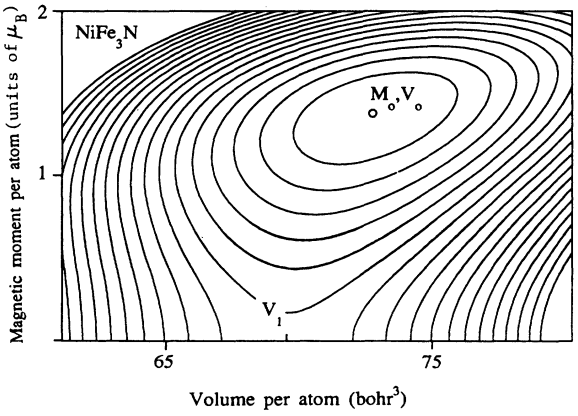

FIG. 5. Fixed-spin-moment (FSM) total-energy surfaces of $NiFe_3N$ as a function of average magnetic moment and volume. M_0 and V_0 denote the ferromagnetic equilibrium values; V_1 is the volume of the nonmagnetic minimum. The distance between two contour lines is 1 mRy/atom.

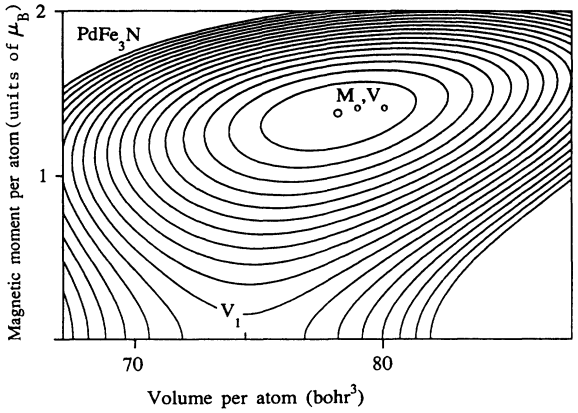

FIG. 6. Fixed-spin-moment (FSM) total-energy surfaces of $PdFe_3N$ (for definitions, see Fig. 5).

which can be seen from the asymmetry and skewing of the contour lines toward larger volumes, an effect more pronounced in the Ni than in the Pd compound. The average magnetic moment per atom is the same for the two compounds, but the magnetic stabilization ΔE_B is by 5.1 mRy/atom (1 mRy/f.u.$\equiv$1.31 kJ/mol) higher in $PdFe_3N$ than in $NiFe_3N$ (Table IV). Both compounds have a very similar value for the magnetovolume coupling constant δ. By calculating the energy contribution of the magnetovolume coupling term for the equilibrium states, we find that the difference in the stabilization energy originates from the larger volume of the Pd system. We have shown (Sec. III B) that the pressure (volume) dependence of the magnetization differs for the two sublattices, and the magnetic properties are essentially determined by iron, while Ni only affects the volume. Furthermore, the volume and magnetic moment per iron are close to the values found for the high-spin state of fcc Fe.[24]

Both compounds show a pronounced difference in volume between the magnetic and nonmagnetic states and have an energy surface similar to that of Fe_3Ni.[14]

TABLE IV. Parameters (top) of the polynomial fit according to Eq. (1), whose units are such that by entering the magnetic moment in μ_B and the volume in bohr^3, the energy is obtained in Ry. Bottom panel: V_0 and M_0 are the volume and magnetic moment of the magnetic equilibrium state, V_1 is the equilibrium volume of the hypothetical nonmagnetic state, and ΔE_B is the difference in total energy (in mRy) between these two states.

	$NiFe_3N$	$PdFe_3N$
A (10^{-1})	0.2534	0.2370
B (10^{-2})	0.2155	0.3680
β (10^{-1})	−0.1837	−0.1749
γ (10^{-3})	0.1320	0.1176
δ (10^{-3})	−0.4589	−0.4798
V_0 (bohr^3)	72.8907	78.2433
V_1 (bohr^3)	69.6205	74.4056
M_0 (μ_B)	1.37	1.37
ΔE_B (mRy)	6.21	11.29

TABLE V. Theoretical magnetomechanical data of $NiFe_3N$ (including experiment) and $PdFe_3N$: a_0 is the equilibrium lattice constant at the temperature stated, P_c is the critical pressure for the disappearance on magnetism, $h=(\partial l/\partial H)/l$ is the forced magnetostriction, α_m is the magnetic contribution to the thermal expansion coefficient (see text), $\partial \ln M/\partial P$ is the pressure derivative of the logarithm of the magnetic moment M, and $\partial T_C/\partial P$ is the pressure derivative of the Curie temperature [assuming (Ref. 23) a Curie temperature of 760 K].

	$NiFe_3N$ theory	$NiFe_3N$ experiment	$PdFe_3N$ theory
a_0 (bohr)	7.143 (0 K)	7.148 (86 K)	7.314 (0 K)
P_c (kbar)	558	530	864
h ($\times 10^{-6}$ T^{-1})	6.7	7.6	11.3
α_m ($\times 10^{-6}$ K^{-1})	−8.61	$5.30-\alpha_{ph}$	−5.00
$\frac{\partial \ln M}{\partial P}$ ($\times 10^{-3}$ kbar^{-1})	−0.90	−1.9	−0.58
$\frac{\partial T_C}{\partial P}$ (K kbar^{-1})	−1.36		

The main difference between Fe-Ni Invar and the present systems is the enhanced stabilization energy ΔE_B between the magnetic and nonmagnetic states. This higher ΔE_B comes mainly from the lattice expansion with respect to the Cu_3Au cell as a result of the insertion of N, but also originates partly from the higher magnetic moments of $NiFe_3N$ and $PdFe_3N$, which are closer to saturation than those of Fe_3Ni.

An important quantity for the occurrence of an Invar behavior is the critical pressure for the disappearance of magnetism, P_c, and related to it, the pressure dependence of Curie temperature and the magnetic moment, $\partial T_C/\partial P$ and $\partial \ln M/\partial P$. Within the framework of spin-fluctuation theory,[15] one obtains the relations

$$P_c=-\frac{2\Delta E_B}{\Delta V_M}\ , \tag{2}$$

$$\frac{dT_C}{dP}=-\frac{T_C}{P_c}\ , \tag{3}$$

$$\frac{\partial \ln M}{\partial P}=-\frac{1}{2}\left[(P_c-P)\left[1-\frac{T}{T_C}\right]\right]^{-1}\ , \tag{4}$$

$$h=M_0/(2V_0P_c)\ \text{ at } T=0\ . \tag{5}$$

In Eq. (2), $\Delta E_B=E(M=0, V_1)-E(M_0, V_0)$ is the energy difference between the nonmagnetic and magnetic states; $\Delta V_M=V_1-V_0$ is the difference of the respective volumes. All quantities entering the calculation of P_c can easily be derived from the fit to the total-energy surface[15] and are given in Table IV. In Eq. (5), M_0 is the equilibrium magnetic moment and V_0 is the respective volume. It should be noted that the Curie temperature depends linearly on pressure (this is in contrast to Stoner theory, where one finds a quadratic power law). Table V summarizes the results and includes a comparison with experiment for $NiFe_3N$, while for $PdFe_3N$ only theoretical values are presented since no experimental data have been found in the literature.

For $NiFe_3N$ the present theory yields a critical pressure of about 558 kbar, which is about 10 times higher than that for Fe_3Ni. Assuming a Curie temperature[25] of about 760 K, one finds dT_C/dP to be -1.36 K kbar.$^{-1}$ Although this value is smaller than for Fe_3Ni ($dT_C/dP\approx -6$ K kbar^{-1}), it is significantly larger than the values for the pure metals, for which one finds almost no pressure dependence of T_C.[26]

The usual explanation why the thermal expansion vanishes (in a certain temperature range) is that the positive phonon contribution of the lattice expansion (Debye term) is compensated by a negative magnetostrictive term (transition from a high-moment high-volume to a low-moment low-volume state). Defining this magnetic contribution α_m as the temperature derivative of the relative lattice expansion $\omega=(l-l_0)/l$, one obtains from spin-fluctuation theory that α_m amounts to -8.61×10^{-6} K^{-1} (for a detailed discussion of the properties of α_m, we refer to Ref. 15). The total thermal-expansion coefficient is obtained by adding the Debye (phonon) contribution α_{ph}. In his recent review on the Invar problem, Wassermann[27] has estimated α_{ph} for Fe_3Ni to be about $+14.0\times 10^{-6}$ K^{-1}. If we assume that α_{ph} remains similar for Fe_3Ni and $NiFe_3N$, we find an overall thermal-expansion coefficient of $+5.4\times 10^{-6}$ K^{-1}, which comes very close to the experimental value of $(5.3-6.0)\times 10^{-6}$ K^{-1} given by Matar *et al.*[9]

V. CONCLUSION

The electronic and magnetic properties of the two compounds $NiFe_3N$ and $PdFe_3N$ were studied by means of band-structure calculations assuming an ordered antiperovskite structure. We found strong covalent bonds between Fe and N which lead to a peak at the Fermi energy, making these compounds weak ferromagnets. The interaction within the metal sublattice is governed by covalent magnetism, where the different exchange splitting for Fe and Ni (Pd) is important. Under pressure the magnetic moment of iron decreases, while that at Ni or Pd stays almost constant or even increases slightly. A similar anomaly is found for the respective hyperfine fields.

Magnetovolume effects at finite temperature were investigated on the basis of these band-structure results by applying a phenomenological spin-fluctuation model. The magnetic contribution to the thermal-expansion coefficient is found to be large and negative, similar to those of the Fe-Ni Invar alloys.

[1]G. W. Wiener and J. A. Berger, J. Met. **7**, 360 (1955).
[2]R. J. Arnott and A. Wold, J. Phys. Chem. Solids **15**, 152 (1960).
[3]J. B. Goodenough, A. Wold, and R. J. Arnott, J. Appl. Phys. **31**, 8342 (1960).
[4]G. Shirane, W. J. Taki, and S. L. Ruby, Phys. Rev. **126**, 49 (1962).
[5]A. Pösinger and W. Steiner (private communication).
[6]B. C. Frazer, Phys. Rev. **112**, 751 (1958).
[7]H. H. Stadelmaier and A. C. Fraker, Trans. Metall. Soc. AIME **218**, 571 (1960).
[8]C. Cordier-Robert and J. Foct, Eur. J. Solid State Inorg. Chem. **29**, 39 (1992).
[9]S. F. Matar, J. G. M. Armitage, P. C. Riedi, G. Demazeau, and P. Hagenmüller, Eur. J. Solid State Inorg. Chem. **26**, 517 (1989).
[10]S. F. Matar, P. Mohn, G. Demazeau, and B. Siberchicot, J. Phys. (Paris) Suppl. **49**, 1761 (1988).
[11]A. R. Williams, J. Kübler, and C. D. Gelatt, Jr., Phys. Rev. B **19**, 6094 (1979).
[12]A. R. Williams, V. L. Moruzzi, J. Kübler, and K. Schwarz, Bull. Am. Phys. Soc. **29**, 278 (1984).
[13]K. Schwarz and P. Mohn, J. Phys. F **14**, L129 (1984).
[14]P. Mohn, K. Schwarz, and D. Wagner, Physica B **161**, 153 (1989).
[15]P. Mohn, K. Schwarz, and D. Wagner, Phys. Rev. B **43**, 3318 (1991).
[16]U. von Barth and L. Hedin, J. Phys. C **5**, 1629 (1972).
[17]J. F. Janak, Solid State Commun. **25**, 53 (1978).
[18]A. R. Williams, R. Zeller, V. L. Moruzzi, C. D. Gelatt, Jr., and J. Kübler, J. Appl. Phys. **52**, 2067 (1981).
[19]J. B. Goodenough, *Magnetism and the Chemical Bond* (Wiley, New York, 1963).
[20]J. Kübler, A. R. Williams, and C. B. Sommers, Phys. Rev. B **28**, 1745 (1983).
[21]T. Dumelow, P. C. Riedi, P. Mohn, K. Schwarz, and Y. Yamada, J. Magn. Magn. Mater. **54-57**, 1081 (1986).
[22]Ch.E. Guillaume, C. R. Acad. Sci. **125**, 235 (1897).
[23]P. Entel and M. Schröter, J. Phys. (Paris) Suppl. **49**, C8-239 (1988).
[24]V. L. Moruzzi, P. M. Marcus, K. Schwarz, and P. Mohn, Phys. Rev. B **34**, 1784 (1986).
[25]S. F. Matar (unpublished).
[26]E. P. Wohlfarth, in *Iron, Cobalt and Nickel,* Vol. 1 of *Ferromagnetic Materials,* edited by E. P. Wohlfarth (North-Holland, Amsterdam, 1980).
[27]E. F. Wassermann, in *INVAR: Moment-Volume Instabilities in Transition Metals and Alloys,* Vol. 5 of *Ferromagnetic Materials,* edited by K. H. Buschow and E. P. Wohlfarth (North-Holland, Amsterdam, 1990).

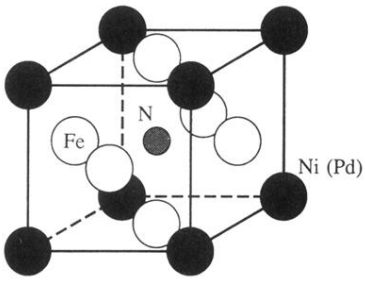

FIG. 1. Antiperovskite structure of $NiFe_3N$ ($PdFe_3N$): with the Ni (Pd) atoms at the corner (solid circles), the Fe atoms at the face center (open circles), and the nitrogen position (hatched circle).